

# Anomalous Relaxation in the $XY$ Gauge Glass

Beom Jun Kim and M.Y. Choi

*Department of Physics and Center for Theoretical Physics  
Seoul National University  
Seoul 151-742, Korea*

S. Ryu and D. Stroud

*Department of Physics  
The Ohio State University  
Columbus, OH 43210*

To study relaxation dynamics of the two-dimensional  $XY$  gauge glass, we integrate directly the equations of motion and investigate the energy function. As usual, it decays exponentially at high temperatures; at low but non-zero temperatures, it is found to exhibit an algebraic relaxation. We compute the relaxation time  $\tau$  as a function of the temperature  $T$  and find that the rapid increase of  $\tau$  at low temperatures is well described by  $\tau \sim (T - T_g)^{-b}$  with  $T_g = 0.22 \pm 0.02$  and  $b = 0.76 \pm 0.05$ , which strongly suggests a finite-temperature glass transition. The decay of vorticity is also examined and explained in terms of a simple heuristic model, which attributes the fast relaxation at high temperatures to annihilation of unpinned vortices.

PACS numbers: 75.10.Nr, 74.50.+r, 74.60.Ge, 61.20.Lc

Recently, dynamics of the physical systems which have many metastable states has drawn much interest [1–3]. In general, such systems show very slow relaxation at low temperatures, where energy barriers separating metastable states are sufficiently high compared with the thermal energy. The  $XY$  gauge glass, which has attracted much attention in relation to the vortex-glass phase of strongly disordered superconductors [4], is a well-known example of the strongly disordered system with a complex energy-landscape. Such a gauge-glass model is of particular interest in two dimensions, with regard to the possible glass order at finite temperatures. Although it is known that the two-dimensional (2D)  $XY$  model with random bond angles does not display a finite-temperature Kosterlitz-Thouless (KT) transition in the strong-disorder regime corresponding to the gauge glass [5], there has been controversy as to the value of the glass transition temperature  $T_g$ : Numerical calculations of the current-voltage ( $IV$ ) characteristics [6] have suggested a zero-temperature transition. However, the temperature range probed in Ref. [6] is not sufficient in view of Ref. [7], where the  $IV$  characteristics appear to indicate a glass transition at lower temperature  $T_g \approx 0.15$ . Further, the analytical result of the vanishing glass-order parameter at finite temperatures [8] does not exclude the possibility of an algebraic *glass* order, characterized by the algebraic decay of the *glass* correlation function (see Ref. [9] for the definition). This is the counterpart of the usual algebraic order (and the associated KT transition) in the 2D pure  $XY$  model, where the Mermin-Wagner theorem [10] does not forbid the existence of such a quasi-long range order, i.e., the algebraic decay of the spin-spin correlation function. Recently, a similar point has been made on the nature of

two-dimensional disordered lattice [11]. Therefore, we believe that the question on the finite-temperature glass transition is not completely settled. Indeed the possibility of algebraic glass order at low temperatures has been suggested in Ref. [12], where it has also been shown that the numerical calculation of the defect-wall energy [13] does not rule out the existence of an algebraic glass order at finite temperatures.

In this work, we study dynamics of the 2D  $XY$  gauge glass in the absence of an external current and investigate the possible glass order at finite temperatures. For this purpose, we consider an array of resistively shunted Josephson junctions with random magnetic bond angles, whose equations of motion are derived from the current conservation condition at each node. Via numerical integration, we compute the energy function and the vorticity function, and find, as expected, that both quantities decay exponentially at high temperatures. In contrast, at low temperatures they are found to exhibit algebraic relaxation: Such striking difference in the decay behaviors according to the temperature  $T$  strongly suggests a dynamical glass transition at a finite temperature  $T_g$ . The behavior of the energy function allows us to estimate the relaxation time  $\tau$ , giving the temperature dependence  $\tau \sim (T - T_g)^{-b}$  with  $T_g = 0.22 \pm 0.02$  and  $b = 0.76 \pm 0.05$ . Whereas  $\tau$  is apparently independent of the system size at sufficiently high temperature ( $T \gg T_g$ ), it increases strikingly with the system size as  $T$  approaches  $T_g$ , manifesting its divergent behavior at  $T = T_g$  in the thermodynamic limit. We also present a simple heuristic model to explain the decay of the vorticity function, and argue that unpinned vortices play an important role in the relaxation behavior.

We begin with an  $L \times L$  square array of resistively

shunted Josephson junctions with periodic boundary conditions in both directions. The net current from grain  $i$  to grain  $j$  is written as the sum of the Josephson current, the normal current, and the thermal noise current:

$$I_{ij} = I_c \sin(\phi_i - \phi_j - A_{ij}) + \frac{V_{ij}}{R} + \Gamma_{ij}, \quad (1)$$

where  $\phi_i$  is the phase of the superconducting order parameter at grain  $i$ ,  $I_c$  is the critical current of the junction,  $V_{ij}$  is the potential difference across the junction, and  $R$  is the shunt resistance. The thermal noise current  $\Gamma_{ij}$  at temperature  $T$  is assumed to satisfy

$$\langle \Gamma_{ij}(t + \tau) \Gamma_{kl}(t) \rangle = \frac{2k_B T}{R} \delta(\tau) (\delta_{ik} \delta_{jl} - \delta_{il} \delta_{jk}), \quad (2)$$

where  $\langle \dots \rangle$  denotes the ensemble average. To describe the gauge glass model, the magnetic bond angles  $A_{ij}$ 's are taken to be quenched random variables distributed uniformly in the interval  $(-\pi, \pi]$ . The potential is related to the phase via the Josephson relation,  $d(\phi_i - \phi_j)/dt = 2eV_{ij}/\hbar$ . This, together with the current conservation at each site, allows us to write Eq. (1) in the form of a set of  $N$  ( $\equiv L^2$ ) coupled equations:

$$\sum_j' \left[ \frac{d}{dt} (\phi_i - \phi_j) + \sin(\phi_i - \phi_j - A_{ij}) + \gamma \eta_{ij} \right] = 0, \quad (3)$$

where the summation is over the nearest neighbors of  $i$  and we have introduced the dimensionless parameter

$$\eta_{ij} \equiv \left( \frac{\hbar I_c}{2ek_B T} \right)^{1/2} \frac{\Gamma_{ij}}{I_c} \equiv \frac{\Gamma_{ij}}{\gamma I_c} \quad (4)$$

and rescaled time  $t$  in units of  $\hbar/(2eRI_c)$ . It is of interest here to note that Eq. (3) describes the *intrinsic* dynamics of the system, based on the current conservation rule. This is in contrast to existing studies of dynamical behaviors, where phenomenological Langevin relaxational dynamics or Glauber dynamics has been adopted, starting from the equilibrium Hamiltonian [1–3].

To study dynamical behaviors, we integrate directly the equations of motion, given by Eq. (3) with  $L = 8, 12, 16$  and  $24$ . In particular, we use random initial conditions with the time step  $\Delta t = 0.05$ , and compute the energy function  $E(t)$ , the auto-correlation function  $C(t)$ , and the vorticity function  $v(t)$ :

$$E(t) \equiv \frac{1}{N} \left\langle \sum_{\langle i,j \rangle} \cos[\phi_i(t) - \phi_j(t) - A_{ij}] \right\rangle, \quad (5)$$

$$C(t) \equiv \left\langle \left| \frac{1}{N} \sum_i e^{i[\phi_i(t) - \phi_i(0)]} \right|^2 \right\rangle, \quad (6)$$

$$v(t) \equiv \frac{1}{N} \left\langle \sum_{\text{all } p} \left| \sum^p [\phi_i(t) - \phi_j(t) - A_{ij}] \right| \right\rangle, \quad (7)$$

where  $\sum_{\langle i,j \rangle}$  is the summation over nearest-neighboring pairs,  $\langle \dots \rangle$  denotes the average over both the initial conditions and disorder configurations. The summation  $\sum^p$  is taken in the counter-clockwise direction over the bonds surrounding plaquette  $p$ , and the phase difference  $\phi_i - \phi_j - A_{ij}$  is defined modulo  $2\pi$ . Since the numerical results are found to be insensitive to the disorder configuration, one realization of  $A_{ij}$  is used in most cases. The auto-correlation function in Eq. (6) measures the time correlation of the glass order parameter; the vorticity function  $v(t)$  in Eq. (7) measures the average chirality on each plaquette regardless of the sign, and is expected to be proportional to the average number density of vortices. In the limit  $t \rightarrow \infty$ , we expect  $E(t)$  and  $v(t)$  should approach the equilibrium values  $E^{eq}$  and  $v^{eq}$ , respectively, at a given temperature  $T$ , while  $C(t)$  approaches  $1/N$  regardless of the temperature (see below).

We first summarize the relaxation behavior of the energy function  $E(t)$ . Figure 1 shows the decay of  $E(t)$  (in units of  $\hbar I_c/2ek_B$ ) of a  $16 \times 16$  array at temperatures (a)  $T = 0.1$  and (b)  $T = 0.6$ . At  $T = 0.1$  it is observed that  $E(t)$  does not achieve its equilibrium value within the time range  $t < 10^5$ , which corresponds to  $2 \times 10^6$  time steps. In particular Fig. 1 (a) shows that for  $t \gtrsim 200$   $E(t)$  fits well with the algebraic decay  $E(t) - E^{eq} \sim t^{-0.30}$ , which is in contrast with the exponential relaxation  $E(t) - E^{eq} \sim \exp(-t/19)$  in Fig. 1 (b). This qualitative change in the relaxation behavior may suggest a finite-temperature glass transition with the glass transition temperature  $T_g$  lower than  $0.6$ . To determine  $T_g$  more precisely, we investigate the normalized energy function

$$\tilde{E}(t) \equiv \frac{E(t) - E^{eq}}{E(t=0) - E^{eq}}, \quad (8)$$

defined to satisfy  $\tilde{E}(0) = 1$  and  $\tilde{E}(t \rightarrow \infty) = 0$ . Since a system with a complicated free energy landscape in general possesses various scales of the relaxation time [14], we write the energy function in the form [14,15]

$$\tilde{E}(t) = \int_0^\infty d\tau' P(\tau') e^{-t/\tau'}, \quad (9)$$

where  $P(\tau')$  describes the distribution of the relaxation time. This gives the average relaxation time  $\tau$  as the integral of the energy function:

$$\tau \equiv \int_0^\infty d\tau' P(\tau') \tau' = \int_0^\infty dt' \tilde{E}(t'). \quad (10)$$

The obtained behavior of  $\tau$  is shown in Fig. 2 for various sizes  $L = 12, 16$ , and  $24$  [16]. It is evident that at high temperatures ( $T \gtrsim 0.5$ ),  $\tau$  is independent of  $L$  within error bars. At low temperatures, on the other hand,  $\tau$  increases with  $L$ . This increase becomes more pronounced as the temperature is lowered, suggesting divergent behavior of  $\tau$  in the thermodynamic limit as  $T$  approaches  $T_g \approx 0.22$  from above. Such a rapid increase

of the average relaxation time as  $T$  is lowered is very well described by the form

$$\tau \sim (T - T_g)^{-b} \quad (11)$$

with the glass-transition temperature  $T_g = 0.22 \pm 0.02$  and the exponent  $b = 0.76 \pm 0.05$ , which is represented by the solid line in Fig. 2. The dotted line in Fig. 2 is the result of the best fit to the form  $\tau \sim T^{-c}$ , i.e., with  $T_g = 0$ : It suggests that the behavior of  $\tau$  is incompatible with the zero-temperature glass transition.

This method of estimating the transition temperature from the average relaxation time has been used in the study of the three-dimensional Ising spin-glass model [15], where both the correlation length in equilibrium and the average relaxation time in dynamics have been shown to diverge at the *same* transition temperature. Indeed a very recent study of the correlation length  $\xi(T)$  for the 2D  $XY$  gauge-glass model showed that  $\xi(T)$  diverges at  $T_g = 0.22 \pm 0.01$  [12], which is consistent with the value obtained dynamically in this work. Here the divergent behavior of the correlation length can be manifested by characteristic finite-size effects in the numerical study performed on a system of finite size: Suppose that the correlation length  $\xi$  diverges at  $T_g$  like  $\xi \sim (T - T_g)^{-\nu}$  with the appropriate exponent  $\nu$ . In the high-temperature regime, the system size  $L$  is in general

much larger than  $\xi$ , and the system is expected not to display appreciable size dependence. Near  $T_g$ , on the other hand, we have  $\xi \gtrsim L$ , which leads to strong finite-size effects.

To examine such behavior, we compute the normalized energy function  $\tilde{E}(t)$  at  $T = 0.6$  and at  $T = 0.25$  and show the results in Fig. 3 and in Fig. 4, respectively. At high temperatures ( $T = 0.6$ ) Fig. 3 shows that the decay of  $\tilde{E}(t)$  does not depend on the system size. In contrast, at low temperatures ( $T = 0.25$ ) the relaxation becomes slower as the size is increased, as displayed in Fig. 4. This size-dependence becomes more distinct as the temperature approaches  $T_g \approx 0.22$  [17]. These different size-dependent behaviors of  $\tilde{E}(t)$  according to the temperature are certainly consistent with the divergence of the correlation length at  $T_g \approx 0.22$ , which indeed supports that both the correlation length in equilibrium and the average relaxation time in dynamics diverge at the *same* transition temperature  $T_g \approx 0.22$ . This estimation is somewhat higher than the value  $T_g \approx 0.15$  estimated from the  $IV$  characteristics [7]. The very slow relaxation at low temperatures makes it difficult to reach the stationary state in numerical simulations, and presumably causes the discrepancy in determining  $T_g$ .

We next investigate the auto-correlation function defined in Eq. (6), which can be cast in the form:

$$\begin{aligned} C(t) &= \left\langle \frac{1}{N^2} \sum_{i,j} \cos[\phi_{ij}(t) - \phi_{ij}(0)] \right\rangle \\ &= \frac{1}{N} + \frac{1}{N^2} \left\langle \sum_{i \neq j} [\cos \phi_{ij}(t) \cos \phi_{ij}(0) + \sin \phi_{ij}(t) \sin \phi_{ij}(0)] \right\rangle \end{aligned} \quad (12)$$

with  $\phi_{ij}(t) \equiv \phi_i(t) - \phi_j(t)$ . At  $t = 0$ , we have the auto-correlation function  $C(t = 0) = \frac{1}{N} + \frac{1}{N^2} N(N - 1) = 1$ . For  $t \rightarrow \infty$ , we expect that  $\phi_{ij}(t)$  and  $\phi_{ij}(0)$  become independent of each other:

$$\langle \cos \phi_{ij}(t) \cos \phi_{ij}(0) \rangle \rightarrow \langle \cos \phi_{ij}(t) \rangle \langle \cos \phi_{ij}(0) \rangle, \quad (13)$$

which, combined with  $\langle \cos \phi_{ij}(0) \rangle = 0$  upon averaging over initial configurations, reveals that  $C(t \rightarrow \infty) = 1/N$  at any temperature. The auto-correlation function obtained numerically at temperatures  $T = 0.1$  and  $0.6$  is plotted in Fig. 5, which shows that approach of  $C(t)$  to the asymptotic value for  $T < T_g$  is qualitatively different from that for  $T > T_g$ .

We finally study the decay of the vorticity function  $v(t)$ , and propose a heuristic model to understand the nature of the transition in terms of annihilation of vortices and antivortices. The vortices present in the system may be classified into three types with regard to their origins: quenched vortices induced by the random bond angle

(type I), thermally generated vortices (type II), and vortices introduced by the random initial conditions (type III). It is plausible to assume that the numbers of vortices and antivortices are equal for each type. Since vortices of type III annihilate as time goes on, only vortices of types I and II exist in equilibrium; thermal vortices (of type II) exist at nonzero temperatures ( $T > 0$ ) [5]. It is further assumed that vortices of type III annihilate with antivortices of the same type or *unpinned* antivortices of types I and II. Since a vortex and an antivortex attract each other, and annihilate when they meet, we suppose that a vortex-antivortex pair with the size (i.e., the distance between the vortex and the antivortex) smaller than  $l$  annihilates after time  $\tilde{t}$ . To obtain the transient behavior of the vorticity function, we consider a vortex configuration consisting of  $n$  antivortices of type III and  $n_0$  unpinned antivortices of types I and II. The average distance  $a$  between the randomly positioned antivortices is given by  $a \approx \sqrt{S/\pi(n + n_0)}$ , where  $S$  is the total area. We now consider a single vortex of type III added at a random po-

sition. The probability  $P$  of the distance between this additional vortex and the nearest antivortex being smaller than  $l$  may be written as  $P \approx \pi l^2/a^2 \approx (\pi^2 l^2/S)(n+n_0)$ , which leads to the decay rate for  $n$  vortices of type III

$$\frac{dn}{dt} \approx -\frac{\pi^2 l^2}{t_0 S} n(n+n_0). \quad (14)$$

Note here that  $n_0$  has been assumed to take its equilibrium value and the fluctuations of  $n_0$  have been neglected. Thus Eq. (14) is valid for  $t$  greater than the ‘‘equilibration’’ time  $t_0$  of  $n_0$  beyond which  $n_0(t)$  reaches its equilibrium value  $n_0$ . It is straightforward to obtain the solution of Eq. (14):  $n(t) = (n_0/2) [\coth(c_1 t + c_2) - 1]$ , where  $c_1 \equiv n_0 \pi^2 l^2 / 2 \bar{t} S$  and  $c_2 \equiv (1/2) \log[1 + n_0/n(\bar{t})] - c_1 \bar{t}$ . The decrease of the vortices of type III results in the relaxation of the vorticity function. Therefore  $n$  is proportional to  $v - v^{eq}$ , and the vorticity function is expected to exhibit the behavior

$$v(t) - v^{eq} \sim [\coth(c_1 t + c_2) - 1], \quad (15)$$

again for  $t$  is larger than  $t_0$ .

We compute numerically the vorticity function, and exhibit the results in Fig. 6 for (a)  $T = 0.1$  and (b)  $T = 0.6$ . At high temperatures ( $T = 0.6$ ), Fig. 6 (b) shows that the numerical data indeed fit very well with Eq. (15) with  $c_1 \approx 0.035$  and  $c_2 \approx 0.087$ , even for rather small  $t$  ( $\gtrsim 1$ ). On the other hand, at low temperatures, the equilibration time  $t_0$  grows large and is expected to be larger than the observation time  $t$ , thus making Eqs. (14) and (15) invalid. In this case the decay of the vorticity function is described by an algebraic function rather than Eq. (15). In Fig. 6 (a), the vorticity function at  $T = 0.1$  is shown to be well described by the algebraic function  $v(t) - v^{eq} \sim t^{-0.41}$ . We have also measured the average relaxation time  $\tau_{\text{vor}}$  of the normalized vorticity function, defined similarly to Eq. (8), and found that it is also divergent near  $T_g$ , again supporting a finite-temperature glass transition.

In summary, we have investigated dynamics of a two-dimensional  $XY$  gauge glass via numerical integration of equations of motion obtained from current conservation conditions. At low temperatures both the energy function and the vorticity function have been found to relax algebraically, which is in contrast with the exponential decay at high temperatures. The auto-correlation function at low temperature has also been shown to relax very slowly. The relaxation time  $\tau$  has been computed and shown to follow  $\tau \sim (T - T_g)^{-0.76}$  with  $T_g = 0.22 \pm 0.02$ . Such divergence of the relaxation time in turn implies the divergence of the correlation length, or slowly (e.g., algebraically) decaying spatial correlations [12]. Finally, the relaxation of the vorticity function has been shown to be closely related to diffusion of unpinned vortices.

BJK and MYC thank S.J. Lee for useful discussions, and acknowledge the partial support from the BSRI Program, Ministry of Education of Korea, and from the

KOSEF through the SRC program. SR and DS was supported in part by the NSF Grant No. DMR94-02131 and by the DOE Grant DE-FG02-90ER-45427.

- 
- [1] For reviews, see, e.g., M. Mezard, G. Parisi, and M.A. Virasoro, *Spin Glass Theory and Beyond* (World Scientific, Singapore, 1986); K. Binder and A.P. Young, *Rev. Mod. Phys.* **58**, 801 (1986).
  - [2] J.J. Mazo, F. Falo, and L.M. Floría, *Phys. Rev. B* **52**, 10433 (1995); D.S. Fisher and D.A. Huse, *Phys. Rev. B* **38**, 373 (1988).
  - [3] H. Rieger, *Physica A* **224**, 267 (1996); *J. Phys A* **26**, L615 (1993).
  - [4] D.S. Fisher and M.P.A. Fisher, and D.A. Huse, *Phys. Rev. B* **43**, 130 (1991).
  - [5] G.S. Jeon, S. Kim, and M.Y. Choi, *Phys. Rev. B* **51**, 16211 (1995).
  - [6] R.A. Hyman, M. Wallin, M.P.A. Fisher, S.M. Girvin, and A.P. Young, *Phys. Rev. B* **51**, 15304 (1995).
  - [7] Y.H. Li, *Phys. Rev. Lett.* **69**, 1819 (1992).
  - [8] H. Nishimori, *Physica A* **205**, 1 (1994).
  - [9] D.A. Huse and H.S. Seung, *Phys. Rev. B* **42**, 1059 (1990).
  - [10] N.D. Mermin and H. Wagner, *Phys. Rev. Lett.* **17**, 1133 (1966).
  - [11] T. Giamarchi and P. Le Doussal, *Phys. Rev. Lett.* **72**, 1530 (1994); *Phys. Rev. B* **52**, 1242 (1995).
  - [12] M.Y. Choi and S.Y. Park, preprint #SNUTP 96-08.
  - [13] M.J.P. Gingras, *Phys. Rev. B* **45**, 7547 (1992); M.P.A. Fisher, T.A. Tokuyasu, and A.P. Young, *Phys. Rev. Lett.* **66**, 2931 (1991).
  - [14] V.S. Dotsenko, *J. Phys. C* **18**, 6023 (1985).
  - [15] A.T. Ogielski and I. Morgenstern, *Phys. Rev. Lett.* **54**, 928 (1985).
  - [16] Numerically, we compute  $\tau(t) \equiv \int_0^t dt' \tilde{E}(t')$  for sufficiently large times at which  $E(t)$  reaches the equilibrium value (i.e.,  $\tilde{E}(t) \approx 0$ ), and take the time-average of  $\tau(t)$  to obtain the average relaxation time. The error bars are then estimated from the fluctuations of  $\tau(t)$  in this large-time regime.
  - [17] These finite-size effects eventually disappear as the size is increased further (so that  $L$  is sufficiently larger than  $\xi(T)$  at the given temperature). For example, we have checked the behavior of  $\tau$  at  $T = 0.3$ , and found that it increases with the size up to  $L = 16$  and then saturates (see Fig. 2).

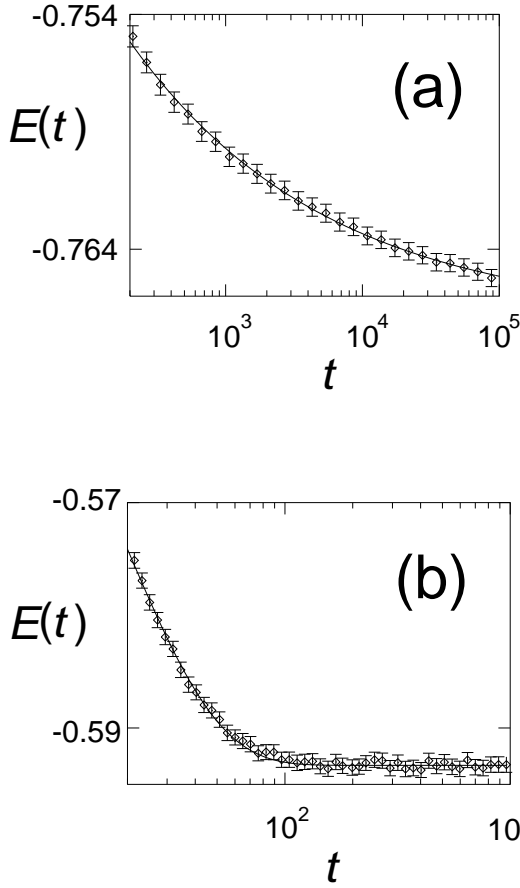


FIG. 1. Relaxation of the energy function at temperatures (a)  $T=0.1$  and (b)  $T=0.6$ . The system size is  $16 \times 16$  and the data have been averaged over more than  $10^3$  samples with different disorder configurations and initial conditions, and error bars correspond to two standard deviations. In (a) the solid line represents the algebraic decay  $E(t) - E^{eq} \sim t^{-0.30}$  with  $E^{eq} = -0.767$ , while the solid line in (b) corresponds to  $E(t) - E^{eq} \sim \exp(-t/19)$  with  $E^{eq} = 0.593$ . As the temperature is decreased, the decay behavior changes from the exponential to the algebraic.

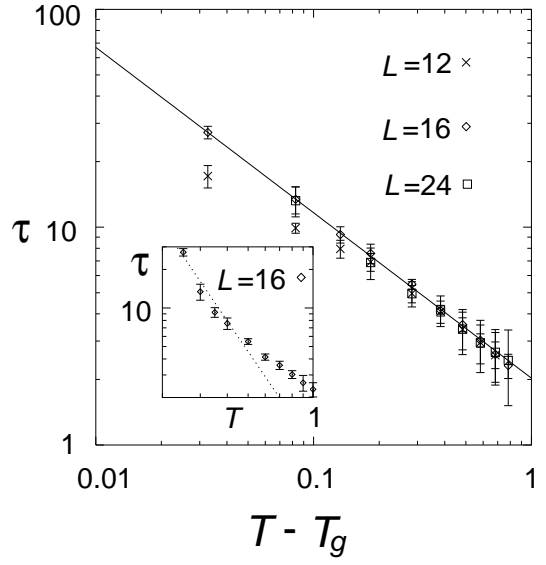


FIG. 2. Relaxation time  $\tau$  versus the temperature  $T - T_g$  in the log-log scale for system sizes  $L = 12, 16,$  and  $24$  with  $T_g = 0.22 \pm 0.02$ . Whereas  $\tau$  is independent of  $L$  at high temperatures, it strongly depends on  $L$  as the temperature is lowered. The rapid increase of  $\tau$  fits well with the form  $(T - T_g)^{-0.76}$ , which is represented by the solid line. Inset:  $\tau$  versus  $T$  in the log-log scale. The dotted line is the result of the least-square fit to the form  $T^{-c}$ , displaying the incompatibility with the zero-temperature glass transition.

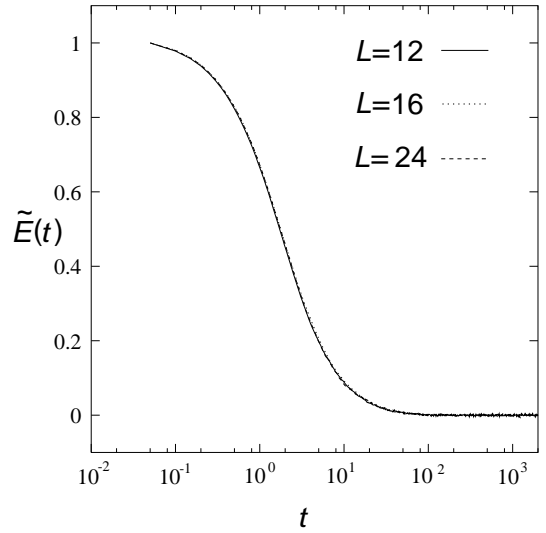


FIG. 3. Relaxation of the normalized energy function  $\tilde{E}$  at temperature  $T = 0.6$ . It is evident that  $\tilde{E}(t)$  is independent of the system size. Typical errors are quite small, of the order of  $10^{-3}$ .

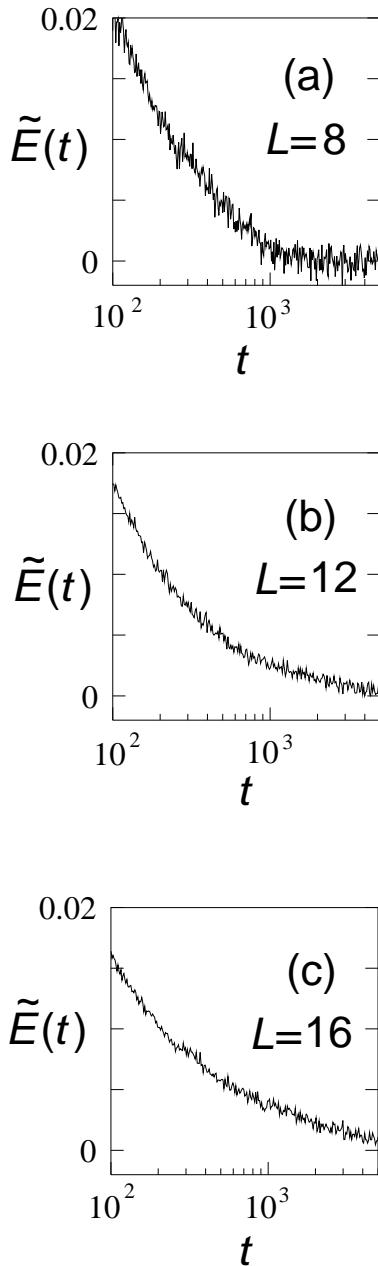


FIG. 4. Relaxation of the normalized energy function  $\tilde{E}$  at temperature  $T = 0.25$  for sizes (a)  $L = 8$ , (b)  $L = 12$ , and (c)  $L = 16$ . As the system size is increased, the relaxation becomes slower.

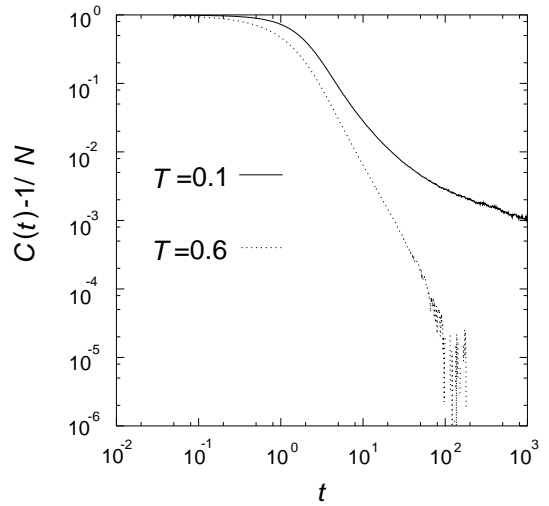


FIG. 5. Relaxation of the auto-correlation function  $C(t)$  at temperatures  $T = 0.1$  and  $0.6$  for  $16 \times 16$  array ( $N = 256$ ). Since  $C(t) \rightarrow 1/N$  as  $t \rightarrow \infty$ ,  $C(t) - 1/N$  is plotted as a function of time  $t$ .

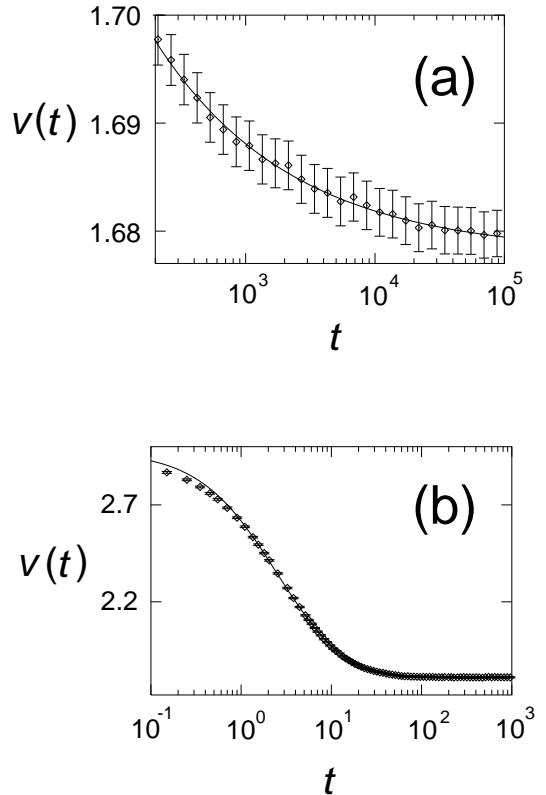


FIG. 6. Relaxation of the vorticity function at temperatures (a)  $T=0.1$  and (b)  $T=0.6$ . The system size and other conditions are the same as those in Fig. 1. In (a) the solid line represents  $v(t) - 1.678 \sim t^{-0.41}$ , while the solid line in (b) corresponds to  $v(t) - 1.702 \sim \coth(0.035t + 0.087) - 1$  [see Eq. (15)]. Note the difference in the vertical scale.